1,2-Dibenzyl- and 1,2-Diaryltetrakis(dimethylamido)dimolybdenum and -ditungsten Compounds: $M_2R_2(NMe_2)_4$ (M≡M). Structural Effects of Me_2N-to-M π Bonding

M. J. Chetcuti, M. H. Chisholm,* K. Folting, D. A. Haitko, J. C. Huffman, and J. Janos

Contribution from the Department of Chemistry and Molecular Structure Center, Indiana University, Bloomington, Indiana 47405. *Received July 15, 1982*

Abstract: From the reactions between RMgCl (R = $CH_2C_6H_5$ and CH_2-*p*-tolyl) or LiR (R = C_6H_5, *p*- and *o*-tolyl) (2 equiv) and 1,2-$M_2Cl_2(NMe_2)_4$ compounds in hydrocarbon solvents, the new compounds 1,2-$M_2R_2(NMe_2)_4$ (M≡M), where M = Mo and W, have been isolated and characterized by a variety of physicochemical techniques. The new compounds, which are air sensitive, hydrocarbon soluble, and diamagnetic, are related to the "ethane-like" dimers previously characterized for R = alkyl. The compound 1,2-$Mo_2(CH_2C_6H_5)_2(NMe_2)_4$ crystallizes in the space group $P2_1/a$ with a = 17.595 (7) Å, b = 16.038 (6) Å, c = 10.542 (4) Å, β = 122.11 (2)°, with Z = 4. Pertinent bond distances and bond angles (averaged) are Mo–Mo = 2.200 (1) Å, Mo–N = 1.95 (1) Å, Mo–C = 2.19 (1) Å, Mo–Mo–N = 104 (1)°, Mo–Mo–C = 100 (1)°. The central $Mo_2N_4C_2$ skeleton has virtual C_2 symmetry (gauche rotamer). The benzyl ligand is σ bonded, not π bonded, as evidenced by equivalent Mo···C_γ distances = 3.7 Å. The compound $Mo_2(p\text{-tolyl})_2(NMe_2)_4$ crystallizes in the anti rotamer: the central $Mo_2N_4C_2$ unit has virtual C_{2h} symmetry. Crystal data are a = 8.046 (2) Å, b = 17.319 (7) Å, c = 18.179 (8) Å, with Z = 4 in the space group *Pcan*. Pertinent bond distances and angles (averaged) are Mo–Mo = 2.196 (1) Å, Mo–N = 1.95 (1) Å, Mo–C = 2.156 (4) Å, Mo–Mo–N = 104 (1)°, Mo–Mo–C = 101.6 (1)°. The compound 1,2-$Mo_2(o\text{-tolyl})_2(NMe_2)_4$ crystallizes in the gauche rotamer and has crystallographically imposed C_2 symmetry. Crystal data are a = 16.845 (4) Å, b = 17.651 (5) Å, c = 8.451 (2) Å, β = 102.74(1)°, with Z = 4 and space group $A2/a$. Pertinent bond distances and angles are Mo–Mo = 2.226 (1) Å, Mo–N = 1.944 (4) Å, Mo–C = 2.169 (4) Å, Mo–Mo–N = 104 (2)°, Mo–Mo–C = 105.0 (1)°. In all three compounds, the Mo–NC_2 units are planar and the NC_2 blades are aligned along the Mo—Mo axis leading to proximal and distal methyl groups. As a result of forming a Mo≡Mo bond, 3 Mo–L σ bonds and 2 Me_2N-to-Mo π bonds, each molybdenum attains 16 valence shell electrons. The preferred alignment of the NC_2 blades along the Mo–Mo axis is determined by the fact that only the in-plane d orbitals ($d_{x^2-y^2}$, d_{xy}) are available for ligand-to-metal π bonding; the d_{z^2}, d_{xz}, and d_{yz} are used to form the Mo≡Mo bond. The σ, rather than π-benzyl, ligand coordination reflects the importance of in-plane Me_2N-to-Mo bonding, as do the relatively high energy barriers observed in solution for rotation about Mo–N bonds, E_{act} ca. 14 kcal mol^{-1}. The lack of π-benzyl coordination along the Mo—Mo axis is also noteworthy and supports the previous suggestion that axial ligation to the $(M{\equiv}M)^{6+}$ unit is not favored. In $Mo_2(p\text{-tolyl})_2(NMe_2)_4$, the aryl ring is aligned along the Mo–Mo axis, but in solution rotation about the Mo–C bond is not frozen out even at −90 °C, 500 MHz. In $Mo_2(o\text{-tolyl})_2(NMe_2)_4$, the aryl ring is aligned perpendicular to the Mo–Mo axis, and ^1H NMR studies support the view that this conformation is also present in solution. These observations provide direct evidence for the importance of Me_2N-to-M π bonding which was previously invoked as a "stabilizing" influence for β-hydrogen-containing alkyl compounds 1,2-$M_2R_2(NMe_2)_4$ (M≡M) where M = Mo and W.

The field of organometallic chemistry has developed largely around soft and π-acceptor ligands such as CO, tertiary phosphines, π olefins and polyenes. Hard π-donor ligands such as oxo, alkoxy, and dialkylamido ligands have received little attention. In early transition-metal chemistry, these ligands could be used to advantage in stabilizing metals in high oxidation states and low or unusual coordination numbers. Electronically these π-donor ligands offer functionality which may buffer changes in coordination number and electron count. They may act as terminal or bridging ligands and their π electrons may occupy bonding or nonbonding molecular orbitals. The stabilization of unusual coordination numbers and geometries by π-donor ligands in the compounds $Mo(CO)_2(O\text{-}t\text{-}Bu)_2(py)_2$ and $Mo(CO)_2(S_2CNR_2)_2$ has attracted the attention of Hoffmann[1] and Templeton[2] and co-workers. We have noted that RO π donors may produce anomalous properties in other ligands which are coordinated to the same metal. For example, in $Mo(CO)_2(O\text{-}t\text{-}Bu)_2(py)_2$,[3] the carbonyl stretching frequencies are anomalously low for carbonyl groups bonded to Mo^{2+}, ν(CO) = 1906 and 1776 cm^{-1}, and in $Mo(O\text{-}i\text{-}Pr)_2(bpy)_2$,[4] the 2,2′-bipyridine ligands appear partially reduced from X-ray and Raman studies. Qualitatively both of these observations may be rationalized in terms of RO-to-Mo π bonding which enhances t_{2g}^4 back-bonding to π^*-acceptor ligands. We have also suggested that the isolation of thermally stable β-hydrogen containing alkyl compounds such as $M_2R_2(NMe_2)_4$ (M≡M), where M = Mo and W,[5] and $TaR(NMe_2)_4$,[6] where R = *t*-Bu and *i*-Pr, is possible because the Me_2N ligands π-donate to metal atomic orbitals which would otherwise be available for mischievous M···H–C interactions. The Me_2N ligands suppress decomposition pathways that might involve an initial β-hydrogen (or α-, γ-) abstraction. The generality of suppressing α-, β-, or γ-H abstraction remains to be established, but it should be noted that Schrock and co-workers[7] have observed a similar effect. Specifically, complexes of the type $M(CHR)L_2X_3$ (M = Nb or Ta, R = CMe_3 or Ph, L = a tertiary phosphine, and X = Cl or Br) react with terminal olefins to give organic products of β-hydride rearrangement of the four possible intermediate metallacyclobutane complexes (no metathesis products or cyclopropanes were observed), whereas with $M(CHCMe_3)(O\text{-}t\text{-}Bu)_2Cl(PMe_3)$ only metathesis products were obtained.

As part of a continuing study of the chemistry surrounding $(M{\equiv}M)^{6+}$ containing compounds (M = Mo and W),[8] we have now prepared 1,2-$M_2R_2(NMe_2)_4$ compounds where R = benzyl and aryl. The conformations and other structural aspects of these

(1) Kubacek, P.; Hoffmann, R. *J. Am. Chem. Soc.* **1981**, *103*, 4320.
(2) Templeton, J. L.; Winston, P. B.; Ward, B. C. *J. Am. Chem. Soc.* **1981**, *103*, 7713.
(3) Chisholm, M. H.; Huffman, J. C.; Kelly, R. L. *J. Am. Chem. Soc.* **1979**, *101*, 7615.
(4) Chisholm, M. H.; Huffman, J. C.; Rothwell, I. P.; Bradley, P. G.; Kress, N.; Woodruff, W. H. *J. Am. Chem. Soc.* **1981**, *103*, 4945.
(5) Chisholm, M. H.; Haitko, D. A.; Folting, K.; Huffman, J. C. *J. Am. Chem. Soc.* **1981**, *103*, 4046.
(6) Chisholm, M. H.; Tan, L. S.; Huffman, J. C. *J. Am. Chem. Soc.* **1982**, *104*, 4879.
(7) Schrock, R. R.; Rocklage, S. M.; Fellman, J. D.; Rupprecht, G. A.; Messerle, L. W. *J. Am. Chem. Soc.* **1981**, *103*, 1440.
(8) Chisholm, M. H.; Cotton, F. A. *Acc. Chem. Res.* **1978**, *11*, 356.

0002-7863/83/1505-1163$01.50/0 © 1983 American Chemical Society

Table I. Analytical and Other Characterization Data for the 1,2-$M_2R_2(NMe_2)_4$ Compounds (M = Mo, W)

compd	color	yield[a]	elemental analyses, % found (calcd) C	H	N
$Mo_2(CH_2Ph)_2(NMe_2)_4$	golden yellow	60	47.77 (48.00)	6.83 (6.95)	10.27 (10.18)
$W_2(CH_2Ph)_2(NMe_2)_4$	brownish yellow	81	36.51 (36.38)	5.08 (5.27)	7.73 (7.71)
$Mo_2(CH_2C_6H_4Me\text{-}4)_2(NMe_2)_4$	yellow	62	49.52 (49.83)	7.20 (7.32)	9.52 (9.68)
$Mo_2Ph_2(NMe_2)_4$	yellow	77	45.85 (45.98)	6.36 (6.56)	10.59 (10.72)
$W_2Ph_2(NMe_2)_4$	orange-yellow	73	34.91 (34.40)	4.99 (4.91)	8.19 (8.02)
$Mo_2(C_6H_4Me\text{-}2)_2(NMe_2)_4$	golden	88	48.06 (48.00)	6.89 (6.95)	10.26 (10.19)
$W_2(C_6H_4Me\text{-}2)_2(NMe_2)_4$	red	80	37.89 (36.38)	5.62 (5.27)	7.57 (7.71)
$Mo_2(C_6H_4Me\text{-}4)_2(NMe_2)_4$	orange	78	47.69 (48.00)	6.77 (6.95)	10.50 (10.18)
$W_2(C_6H_4Me\text{-}4)_2(NMe_2)_4$	brick-red	84	36.89 (36.38)	5.62 (5.27)	7.57 (7.71)

[a] Percent yield based on eq 1.

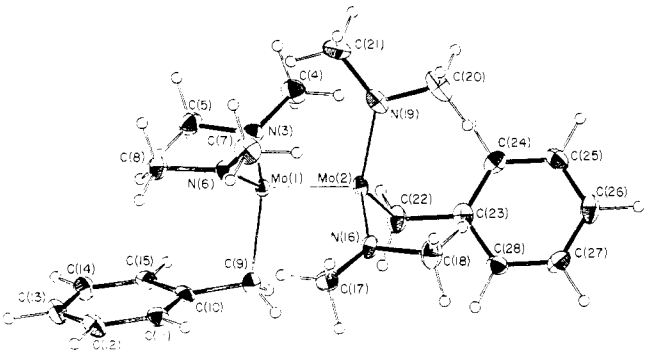

Figure 1. ORTEP view of the 1,2-$Mo_2(benzyl)_2(NMe_2)_4$ molecule showing the atom number scheme.

new compounds provide unequivocal evidence for the dominant role of Me_2N-to-M π bonding in these types of complexes.

Results and Discussion

Syntheses. The new compounds may be prepared by the general synthesis outlined in eq 1, for R = $CH_2C_6H_5$, CH_2-*p*-tolyl, phenyl,

$$1,2\text{-}M_2Cl_2(NMe_2)_4 + 2LiR \xrightarrow[20\ °C]{hexane} 1,2\text{-}M_2R_2(NMe_2)_4 + 2LiCl \quad (1)$$

and *o*- and *p*-tolyl and M = Mo or W. An alternative synthesis using benzyl Grignard reagents has been used equally well for the synthesis of the benzyl compounds. The reactions proceed smoothly at room temperature and appear complete within 2–3 h. Slow filtration using Celite and a fine frit yields hexane extracts which, upon reduction in volume of the solvent and cooling, give $M_2R_2(NMe_2)_4$ as crystalline products in high yields, ca. 70–80% based on eq 1. Elemental analyses and other characterization data are given in Table I. The compounds are air sensitive and must be handled in dry and oxygen-free atmospheres and solvents. They are more soluble in toluene and benzene than in hexane and alkane solvents. The general solubility trend for these compounds is R = alkyl > benzyl > *o*- and *p*-tolyl > phenyl. When heated in vacuo, these compounds sublime, but with decomposition. Purification by recrystallization is preferred to sublimation. In the mass spectrometer, $M_2R_2(NMe_2)_4^+$ ions along with many other M_2-containing ions are observed. ^1H NMR data and IR data are recorded in the Experimental Section.

Solid-State and Molecular Structures. *gauche*-1,2-$Mo_2(CH_2Ph)_2(NMe_2)_4$. An ORTEP view of the *gauche*-$Mo_2(CH_2Ph)_2(NMe_2)_4$ molecule found in the crystal is shown in Figure 1. The molecule has virtual, but not crystallographically imposed, C_2 symmetry. Indeed, it is interesting to note that the $Mo_2(NC_2)_4$ skeleton has near perfect C_2 symmetry, and it is only benzyl ligands which differ slightly with respect to each end of the molecule. This effect is clearly apparent from an inspection of the stereoviews shown in Figure 2 in which the two halves of the molecule related by the virtual C_2 axis of symmetry are superimposed. A view of the molecule looking down the Mo–Mo axis is shown in Figure 3. This view shows how the planar Mo–NC_2 units are aligned coincident with the Mo–Mo axis; it also shows the orientation of the phenyl group with respect to the Mo–C bonds.

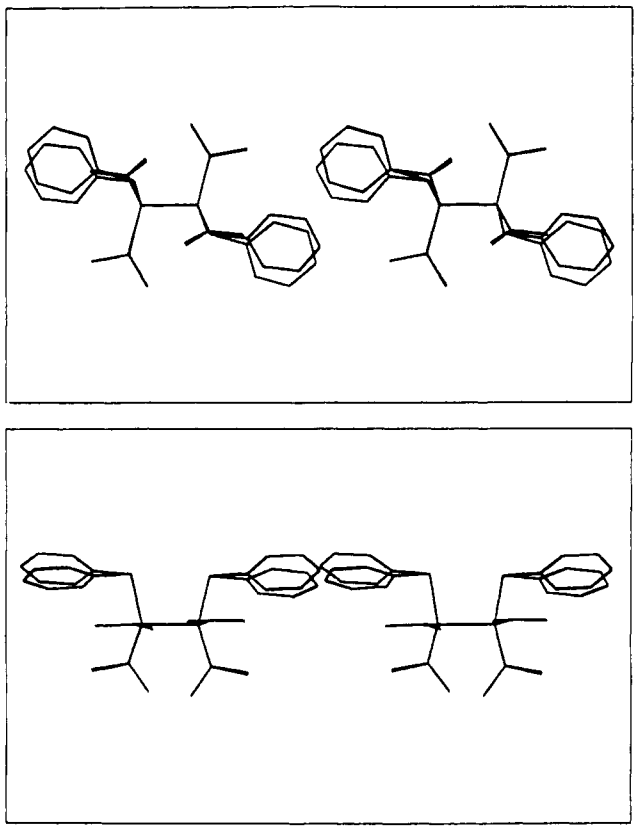

Figure 2. Two stereoviews of the $Mo_2(benzyl)_2(NMe_2)_4$ emphasizing the virtual, but not absolute, C_2 element of symmetry. The operation of a C_2 rotation about the virtual C_2 axis produces significant mismatch of the phenyl carbons but has a minimal effect on the $Mo_2(C)_2(NC_2)_4$ skeleton of the molecule.

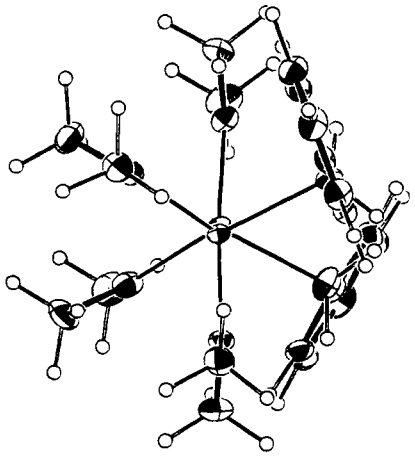

Figure 3. ORTEP view of the $Mo_2(benzyl)_2(NMe_2)_4$ molecule looking down the Mo–Mo bond.

Table II. Fractional Coordinates and Isotropic Thermal Parameters for the 1,2-$Mo_2(benzyl)_2(NMe_2)_4$ Molecule[a]

atom	x	y	z	B_{iso}
Mo(1)	1046.0 (2)	1790.5 (2)	−473.2 (4)	11
Mo(2)	−143.4 (2)	1873.1 (2)	−2757.7 (4)	13
N(3)	571 (2)	1718 (2)	824 (4)	15
C(4)	−323 (3)	1791 (3)	580 (6)	24
C(5)	1239 (3)	1685 (3)	2437 (5)	22
N(6)	1778 (2)	2735 (2)	−350 (4)	16
C(7)	1619 (4)	3447 (3)	−1326 (6)	26
C(8)	2633 (3)	2834 (3)	1081 (6)	22
C(9)	1601 (3)	592 (3)	−626 (5)	15
C(10)	2532 (3)	592 (3)	670 (5)	15
C(11)	3240 (3)	879 (3)	554 (5)	18
C(12)	4114 (3)	899 (3)	1778 (6)	22
C(13)	4305 (3)	632 (3)	3178 (6)	23
C(14)	3604 (3)	349 (3)	3311 (5)	20
C(15)	2741 (3)	326 (3)	2090 (5)	17
N(16)	349 (2)	1845 (2)	−4040 (4)	16
C(17)	1245 (3)	1905 (3)	−3775 (5)	21
C(18)	−328 (4)	1907 (3)	−5648 (5)	26
N(19)	−759 (3)	2865 (3)	−2683 (4)	21
C(20)	−1580 (4)	3099 (4)	−4077 (7)	31
C(21)	−486 (4)	3525 (3)	−1557 (6)	27
C(22)	−800 (3)	700 (3)	−2852 (5)	22
C(23)	−1671 (3)	688 (3)	−4292 (5)	18
C(24)	−2444 (3)	1058 (3)	−4469 (5)	19
C(25)	−3251 (3)	1061 (3)	−5830 (6)	21
C(26)	−3324 (3)	700 (3)	−7081 (5)	23
C(27)	−2569 (3)	336 (3)	−6944 (6)	23
C(28)	−1765 (3)	329 (3)	−5584 (5)	19

[a] Fractional coordinates are $\times 10^4$. B_{iso} values are $\times 10$. Isotropic values for those atoms refined anisotropically are calculated with the formula given by Hamilton (Hamilton, W. C. *Acta Crystallogr.* **1959**, *12*, 609).

Table III. Bond Distances (Å) for the 1,2-$Mo_2(benzyl)_2(NMe_2)_4$ Molecule

A	B	distance	A	B	distance
Mo(1)	Mo(2)	2.200 (1)	C(9)	C(10)	1.474 (6)
Mo(1)	N(3)	1.949 (3)	C(10)	C(11)	1.392 (6)
Mo(1)	N(6)	1.948 (4)	C(10)	C(15)	1.404 (6)
Mo(1)	C(9)	2.201 (5)	C(11)	C(12)	1.386 (7)
Mo(2)	N(16)	1.956 (4)	C(12)	C(13)	1.396 (7)
Mo(2)	N(19)	1.949 (4)	C(13)	C(14)	1.390 (7)
Mo(2)	C(22)	2.182 (5)	C(14)	C(15)	1.373 (6)
N(3)	C(4)	1.457 (6)	C(22)	C(23)	1.477 (6)
N(3)	C(5)	1.466 (6)	C(23)	C(24)	1.402 (6)
N(6)	C(7)	1.462 (6)	C(23)	C(28)	1.405 (7)
N(6)	C(8)	1.466 (6)	C(24)	C(25)	1.382 (7)
N(16)	C(17)	1.451 (6)	C(25)	C(26)	1.382 (7)
N(16)	C(18)	1.467 (6)	C(26)	C(27)	1.386 (7)
N(19)	C(20)	1.460 (6)	C(27)	C(28)	1.379 (7)
N(19)	C(21)	1.468 (7)			

Final atomic positional parameters are given in Table II. Listings of bond distances and angles are given in Tables III and IV, respectively. Many of these are expected in view of the previously characterized $Mo_2Me_2(NMe_2)_4$[9] and $Mo_2Et_2(NMe_2)_4$[5] compounds.

The Mo–C (benzyl) distance, 2.19 (1) Å (averaged), is a perfectly respectable Mo–Csp^3 distance and may be compared with the related Mo–C (ethyl) distances of 2.165 (6) Å and 2.21 (1) Å (averaged) found in $Mo_2Et_2(NMe_2)_4$[5] and $Mo_2Et_2(NMe_2)_2(C_7H_7N_3C_7H_7)_2$.[10] Furthermore, the Mo–C–C angles, 104.5 (4)° and 107.1 (3)°, are close to idealized tetrahedral angles. That the benzyl ligand is σ bonded (η^1) rather than π bonded (η^3) is evident from the consideration of the following distances: Mo(1)–C(10), –C(11), –C(15) = 2.94 (1), 3.71 (1), and 3.63 (1) Å, and Mo(2)–C(23), –C(24), –C(28) = 2.97 (1), 3.69 (1), and 3.76 (1) Å, respectively. The two Mo···C(γ) distances for each Mo–benzyl group are roughly equal and at 3.7 Å, too long to allow for any π-allylic bonding. These distances may be compared to Mo–C(α) = 2.269 (7) Å, Mo–C(β) = 2.364 (5) Å, Mo–C(γ) = 2.480 (6) Å, and Mo···C(γ′) (nonbonded) = 3.307 (6) Å for the first structurally characterized η^3-benzylmolybdenum complex, $(CH_3C_6H_4CH_2)(C_5H_5)Mo(CO)_2$.[11] Qualitatively, the lack of any π-benzylic bonding or multicenter (aliphatic) C–H···Mo bonding in $Mo_2(CH_2Ph)_2(NMe_2)_4$ may be surmised by inspection of the view of the molecule shown in Figure 3.

Table IV. Bond Angles (deg) for the 1,2-$Mo_2(benzyl)_2(NMe_2)_4$ Molecule

A	B	C	angle
Mo(2)	Mo(1)	N(3)	105.0 (1)
Mo(2)	Mo(1)	N(6)	103.7 (1)
Mo(2)	Mo(1)	C(9)	100.0 (1)
N(3)	Mo(1)	N(6)	121.0 (2)
N(3)	Mo(1)	C(9)	111.8 (2)
N(6)	Mo(1)	C(9)	112.4 (2)
Mo(1)	Mo(2)	N(16)	104.0 (1)
Mo(1)	Mo(2)	N(19)	103.3 (1)
Mo(1)	Mo(2)	C(22)	99.8 (1)
N(16)	Mo(2)	N(19)	120.4 (2)
N(16)	Mo(2)	C(22)	111.5 (2)
N(19)	Mo(2)	C(22)	114.4 (2)
Mo(1)	N(3)	C(4)	134.1 (3)
Mo(1)	N(3)	C(5)	116.0 (3)
C(4)	N(3)	C(5)	109.4 (4)
Mo(1)	N(6)	C(7)	133.5 (3)
Mo(1)	N(6)	C(8)	115.7 (3)
C(7)	N(6)	C(8)	110.3 (4)
Mo(2)	N(16)	C(17)	134.4 (3)
Mo(2)	N(16)	C(18)	114.3 (3)
C(17)	N(16)	C(18)	110.5 (4)
Mo(2)	N(19)	C(20)	116.4 (4)
Mo(2)	N(19)	C(21)	132.2 (3)
C(20)	N(19)	C(21)	110.5 (4)
Mo(1)	C(9)	C(10)	104.5 (3)
C(9)	C(10)	C(11)	121.6 (4)
C(9)	C(10)	C(15)	121.4 (4)
C(11)	C(10)	C(15)	117.0 (4)
C(10)	C(11)	C(12)	121.9 (4)
C(11)	C(12)	C(13)	120.1 (4)
C(12)	C(13)	C(14)	118.6 (4)
C(13)	C(14)	C(15)	120.8 (4)
C(10)	C(15)	C(14)	121.6 (4)
Mo(2)	C(22)	C(23)	107.1 (3)
C(22)	C(23)	C(24)	122.3 (4)
C(22)	C(23)	C(28)	121.6 (4)
C(24)	C(23)	C(28)	116.0 (4)
C(23)	C(24)	C(25)	121.9 (4)
C(24)	C(25)	C(26)	120.8 (4)
C(25)	C(26)	C(27)	118.7 (4)
C(26)	C(27)	C(28)	120.6 (4)
C(23)	C(28)	C(27)	122.1 (4)

***anti*-1,2-Mo_2(*p*-Tolyl)$_2(NMe_2)$.** An ORTEP view of the *anti*-1,2-Mo_2(*p*-tolyl)$_2(NMe_2)_4$ molecule found in the solid state is shown in Figure 4. The molecule has virtual C_{2h} symmetry and rigorous (crystallographically imposed) C_2 symmetry. The view shown in Figure 4 is down the C_2 axis of symmetry. A view of the molecule looking down the Mo–Mo axis is shown in Figure 5. This view shows that the NC_2 blades and the phenyl rings are aligned along the Mo–Mo axis.

Final atomic positional parameters are given in Table V and listings of bond distances and angles are given in Tables VI and VII.

The Mo≡Mo, Mo–N, and M–C (tolyl) bond distances and the $Mo_2N_4C_2$ angles are all entirely consistent with what one might have anticipated. The Mo–N(sp^2) distances are shorter than the

(9) Chisholm, M. H.; Cotton, F. A.; Extine, M. W.; Murillo, C. A. *Inorg. Chem.* **1978**, *17*, 2338.

(10) Chetcuti, M. J.; Chisholm, M. H.; Haitko, D. A.; Folting, K.; Huffman, J. C. *J. Am. Chem. Soc.* **1982**, *104*, 2138.

(11) Cotton, F. A.; LaPrade, M. D. *J. Am. Chem. Soc.* **1968**, *90*, 5418. For a recent discussion of structural aspects of π-benzylic complexes, see ref 12 and references cited therein.

(12) Busch, R. R.; Muetterties, E. L.; Day, V. W. *Organometallics* **1982**, *1*, 188.

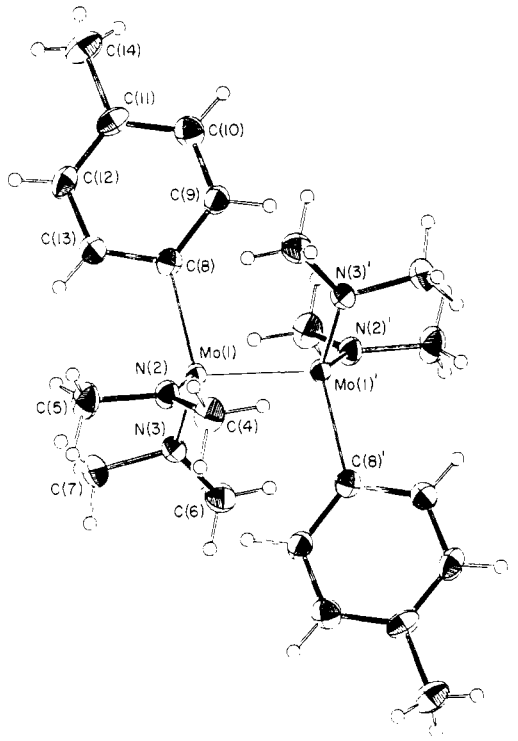

Figure 4. ORTEP view of the 1,2-$Mo_2(p\text{-tolyl})_2(NMe_2)_4$ molecule showing the atom number scheme.

Table V. Fractional Coordinates and Isotropic Thermal Parameters for the $Mo_2(p\text{-tolyl})_2(NMe_2)_4$ Molecule[a]

atom	x	y	z	B_{iso}
Mo(1)	4335.0 (4)	4516.2 (2)	−256.4 (2)	14
N(2)	2927 (4)	5012 (2)	−985 (2)	19
N(3)	6098 (4)	3812 (2)	−566 (2)	18
C(4)	2828 (6)	5796 (3)	−1270 (3)	26
C(5)	1888 (6)	4492 (3)	−1424 (2)	29
C(6)	7893 (6)	3834 (3)	−539 (3)	26
C(7)	5544 (6)	3173 (2)	−1026 (2)	25
C(8)	2964 (5)	4057 (2)	664 (2)	18
C(9)	2846 (5)	4324 (2)	1391 (2)	20
C(10)	1973 (6)	3932 (2)	1927 (2)	24
C(11)	1146 (5)	3249 (2)	1765 (2)	22
C(12)	1230 (5)	2976 (2)	1051 (2)	23
C(13)	2116 (5)	3374 (2)	521 (2)	22
C(14)	210 (8)	2818 (3)	2349 (3)	34

[a] Fractional coordinates are $\times 10^4$. B_{iso} values are $\times 10$. Isotropic values for those atoms refined anisotropically are calculated with the formula given by Hamilton (Hamilton, W. C. *Acta Crystallogr.* **1959**, *12*, 609).

Table VI. Bond Distances (Å) for the $Mo_2(p\text{-tolyl})_2(NMe_2)_4$ Molecule

A	B	distance	A	B	distance
Mo(1)	Mo(1)'	2.196 (1)	C(8)	C(9)	1.404 (5)
Mo(1)	N(2)	1.943 (3)	C(8)	C(13)	1.390 (5)
Mo(1)	N(3)	1.954 (3)	C(9)	C(10)	1.379 (6)
Mo(1)	C(8)	2.156 (4)	C(10)	C(11)	1.389 (6)
N(2)	C(4)	1.457 (5)	C(11)	C(12)	1.383 (6)
N(2)	C(5)	1.465 (5)	C(11)	C(14)	1.500 (6)
N(3)	C(6)	1.445 (5)	C(12)	C(13)	1.383 (6)
N(3)	C(7)	1.456 (5)			

Mo–C(sp^2) distances by 0.2 Å. It is safe to say that there is little, if any, Mo–tolyl π bonding, and so the markedly shorter Mo–N distances reflect the high degree of Me_2N-to-Mo π bonding. In the limit, this may be counted as a double bond, M=NMe_2.

***gauche*-1,2-$Mo_2(o\text{-Tolyl})_2(NMe_2)_4$.** In the space group $A2/a$, the *gauche*-1,2-$Mo_2(o\text{-tolyl})_2(NMe_2)_4$ molecule has crystallographically imposed C_2 symmetry. An ORTEP view of the molecule viewed down the C_2 axis is shown in Figure 6, and a view looking down the Mo–Mo axis is shown in Figure 7. Quite strikingly, the aryl plane is virtually perpendicular to the Mo–Mo–C plane. The aryl ring in the *o*-tolyl compound is rotated 90° from the alignment found for the *p*-tolyl ligand in 1,2-$Mo_2(p\text{-tolyl})_2(NMe_2)_4$.

Table VII. Bond Angles (deg) for the $Mo_2(p\text{-tolyl})_2(NMe_2)_4$ Molecule

A	B	C	angle
Mo(1)'	Mo(1)	N(2)	103.7 (1)
Mo(1)'	Mo(1)	N(3)	104.2 (1)
Mo(1)'	Mo(1)	C(8)	101.6 (1)
N(2)	Mo(1)	N(3)	120.2 (1)
N(2)	Mo(1)	C(8)	113.2 (1)
N(3)	Mo(1)	C(8)	111.4 (1)
Mo(1)	N(2)	C(4)	133.4 (3)
Mo(1)	N(2)	C(5)	115.7 (3)
C(4)	N(2)	C(5)	110.3 (3)
Mo(1)	N(3)	C(6)	134.3 (3)
Mo(1)	N(3)	C(7)	114.7 (3)
C(6)	N(3)	C(7)	110.3 (3)
Mo(1)	C(8)	C(9)	130.1 (3)
Mo(1)	C(8)	C(13)	114.9 (3)
C(9)	C(8)	C(13)	115.0 (3)
C(8)	C(9)	C(10)	122.5 (4)
C(9)	C(10)	C(11)	120.9 (4)
C(10)	C(11)	C(12)	117.8 (4)
C(10)	C(11)	C(14)	121.0 (4)
C(12)	C(11)	C(14)	121.2 (4)
C(11)	C(12)	C(13)	120.6 (4)
C(8)	C(13)	C(12)	123.2 (4)

Table VIII. Fractional Coordinates and Isotropic Thermal Parameters for the 1,2-$Mo_2(o\text{-tolyl})_2(NMe_2)_4$ Molecule[a]

atom	x	y	z	B_{iso}
Mo(1)	3160.7 (2)	4722.8 (2)	0.9 (3)	11
N(2)	3723 (2)	4629 (2)	2261 (3)	16
C(3)	4602 (2)	4524 (3)	2533 (5)	22
C(4)	3478 (2)	4572 (3)	3796 (5)	24
N(5)	3275 (2)	3868 (2)	−1384 (4)	15
C(6)	4102 (2)	3722 (2)	−1596 (5)	19
C(7)	2748 (2)	3224 (2)	−1987 (5)	21
C(8)	3380 (2)	5807 (2)	−1032 (4)	14
C(9)	3331 (2)	5843 (2)	−2714 (5)	18
C(10)	3568 (2)	6467 (2)	−3484 (5)	21
C(11)	3890 (2)	7088 (2)	−2576 (5)	23
C(12)	3943 (2)	7079 (2)	−916 (5)	22
C(13)	3692 (2)	6461 (2)	−131 (4)	17
C(14)	3755 (3)	6504 (2)	1673 (5)	22

[a] Fractional coordinates are $\times 10^4$. B_{iso} values are $\times 10$. Isotropic values for those atoms refined anisotropically are calculated using the formula given by Hamilton (Hamilton, W. C. *Acta Crystallogr.* **1959**, *12*, 609).

Table IX. Bond Distances (Å) for the 1,2-$Mo_2(o\text{-tolyl})_2(NMe_2)_4$ Molecule

A	B	distance	A	B	distance
Mo(1)	Mo(1)'	2.226 (1)	C(8)	C(9)	1.407 (5)
Mo(1)	N(2)	1.943 (3)	C(8)	C(13)	1.418 (5)
Mo(1)	N(5)	1.945 (3)	C(9)	C(10)	1.382 (5)
Mo(1)	C(8)	2.169 (4)	C(10)	C(11)	1.380 (6)
N(2)	C(3)	1.460 (4)	C(11)	C(12)	1.385 (6)
N(2)	C(4)	1.448 (5)	C(12)	C(13)	1.391 (5)
N(5)	C(6)	1.465 (4)	C(13)	C(14)	1.507 (5)
N(5)	C(7)	1.463 (5)			

Final atomic positional parameters are given in Table VIII, and listings of bond distances and angles are given in Tables IX and X, respectively. The introduction of the more sterically demanding *o*-tolyl ligand causes certain systematic, though small changes in distances and angles from those associated with the *p*-tolyl compound. The Mo–Mo distance, 2.226 (1) Å, is 0.03 Å longer; the Mo–C distance, 2.169 (4) Å, is 0.01 Å longer. The Mo–Mo–C

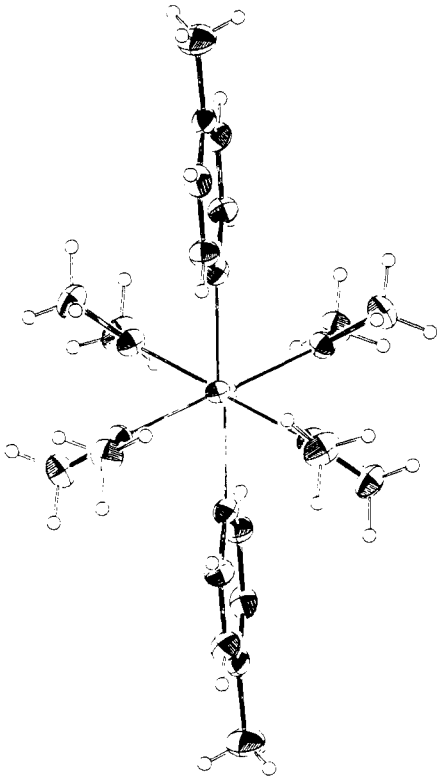

Figure 5. ORTEP view of the 1,2-$Mo_2(p\text{-tolyl})_2(NMe_2)_4$ molecule viewed down the Mo–Mo bond.

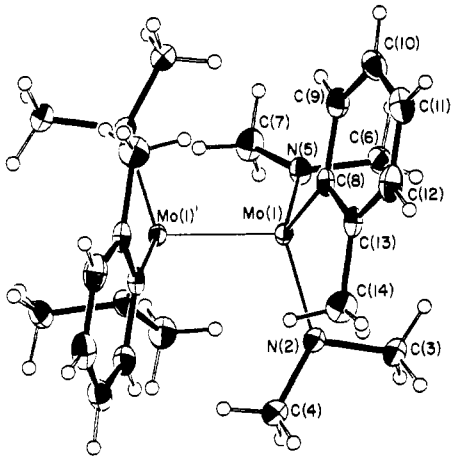

Figure 6. ORTEP view of the 1,2-$Mo_2(o\text{-tolyl})_2(NMe_2)_4$ molecule viewed down the C_2 axis of symmetry and showing the atom number scheme used in the tables.

angle of 105.0° in the *o*-tolyl complex is larger than that in the *p*-tolyl complex (101.6°) while the N–Mo–N angle is correspondingly smaller, 115.7° (*o*-tolyl) compared to 120.2° (*p*-tolyl), as would be expected in order to accommodate the "sideways" or "perpendicular" conformation of the aromatic ring.

^{1}H NMR Studies. 1,2-$M_2(Benzyl)_2(NMe_2)_4$ Compounds. In toluene-d_8 solutions, the $M_2(benzyl)_2(NMe_2)_4$ compounds show the presence of both anti and gauche rotamers with the gauche being preferred roughly 5:1. The methylene protons of the anti rotamer appear as a singlet while for the gauche rotamer thay appear as an AB quartet which is consistent with expectations based on symmetry. Significantly, there appears to be free (unrestricted) rotation about Mo–C and C–C (phenyl) bonds on the NMR time scale which is in line with the view that the benzyl ligands are not σ (not π) bonded. By contrast, rotations about Mo–N bonds are slow at low temperatures on the NMR time scale, and at −45 °C, 220 MHz, low-temperature limiting ^{1}H NMR spectra are obtained which are consistent with frozen out

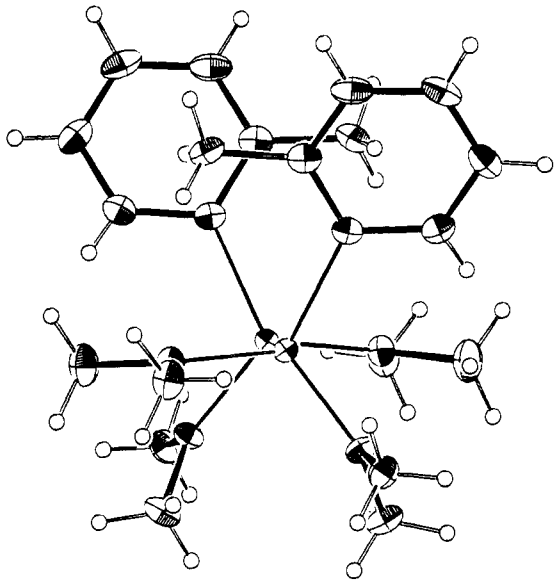

Figure 7. ORTEP view of the 1,2-$Mo_2(o\text{-tolyl})_2(NMe_2)_4$ molecule looking down the Mo–Mo axis.

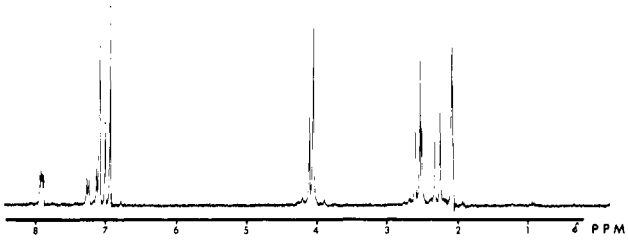

Figure 8. Low-temperature limiting spectra of an equilibrium mixture of *anti*- and *gauche*-1,2-$Mo_2(p\text{-tolyl})_2(NMe_2)_4$ recorded at −45 °C in toluene-d_8 at 220 MHz. Protium impurities in the toluene-d_8 give rise to signals denoted by an asterisk.

Table X. Bond Angles (deg) for the 1,2-$Mo_2(o\text{-tolyl})_2(NMe_2)_4$ Molecule

A	B	C	angle
Mo(1)'	Mo(1)	N(2)	105.7 (1)
Mo(1)'	Mo(1)	N(5)	103.4 (1)
Mo(1)'	Mo(1)	C(8)	105.0 (1)
N(2)	Mo(1)	N(5)	115.7 (1)
N(2)	Mo(1)	C(8)	112.5 (1)
N(5)	Mo(1)	C(8)	113.2 (1)
Mo(1)	N(2)	C(3)	115.0 (2)
Mo(1)	N(2)	C(4)	135.5 (2)
C(3)	N(2)	C(4)	109.3 (3)
Mo(1)	N(5)	C(6)	115.6 (2)
Mo(1)	N(5)	C(7)	132.8 (2)
C(6)	N(5)	C(7)	110.0 (3)
Mo(1)	C(8)	C(9)	117.9 (3)
Mo(1)	C(8)	C(13)	125.3 (3)
C(9)	C(8)	C(13)	116.0 (3)
C(8)	C(9)	C(10)	123.5 (4)
C(9)	C(10)	C(11)	119.4 (4)
C(10)	C(11)	C(12)	118.9 (4)
C(11)	C(12)	C(13)	122.2 (4)
C(8)	C(13)	C(12)	119.9 (3)
C(8)	C(13)	C(14)	121.3 (3)
C(12)	C(13)	C(14)	118.8 (4)

proximal and distal *N*-methyl groups. At high temperatures, >45 °C, proximal ⇌ distal *N*-methyl exchange is fast on the ^{1}H NMR time scale, but anti ⇌ gauche isomerization is not. For compounds of the type 1,2-$M_2X_2(NR_2)_4$, where R = Me or Et and X = Me or CH_2SiMe_3, the latter process has been shown[13] to have an

(13) Chisholm, M. H.; Cotton, F. A.; Extine, M. W.; Millar, M. *Inorg. Chem.* **1977**, *16*, 320.

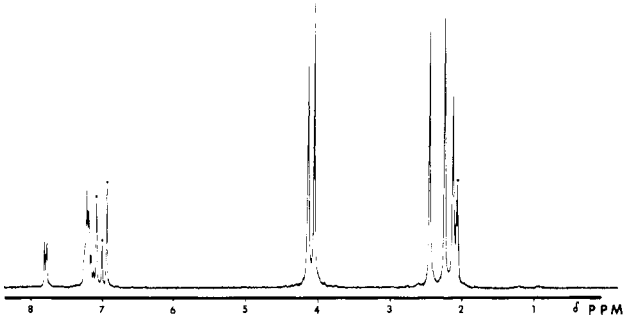

Figure 9. ^{1}H NMR spectrum of *gauche*-1,2-Mo_2(*o*-tolyl)$_2$(NMe_2)$_4$ recorded at −50 °C, 220 MHz in toluene-d_8 solvent. Signals arising from protium impurities in toluene-d_8 are denoted by an asterisk.

energy of activation of ca. 24 kcal mol^{-1}.

1,2-M_2(Aryl)$_2$(NMe_2)$_4$ Compounds. The ^{1}H NMR spectra recorded in toluene-d_8 in the temperature range −80 °C to +85 °C for the phenyl and *p*-tolyl compounds were as expected for a mixture of anti and gauche rotamers with proximal ⇌ distal *N*-methyl exchange being frozen out at low temperatures. The low-temperature limiting spectrum for the *p*-tolyl compound is shown in Figure 8. The ^{1}H signals for the ortho and meta hydrogens fall into two types which, by comparison with the integral intensity of the *N*-methyl groups, may be assigned to anti and gauche molecules. Significantly, these signals shown little temperature dependence which, in view of the large diamagnetic anisotropy associated with the M≡M bond[14] and the positioning of the ortho protons seen in the solid state for the anti rotamer, suggests a very low barrier to rotation about the Mo–C (aryl) bonds. Even at 500 MHz and −90 °C, the spectrum showed no evidence for restricted rotation about these bonds. This observation prompted us to prepare the *o*-tolyl compound: the *o*-methyl group was expected to have a site preference either proximal or distal (the latter seeming more likely) to the M≡M bond. A further check on McGlinchey's[14] calculation of $\chi_{M\equiv M}$ for M = Mo and W would be interesting for these types of compounds. Although the synthesis of the *o*-tolyl compounds was straightforward, the ^{1}H NMR spectra revealed the presence of only the gauche rotamer in solution. See Figure 9. Furthermore, the signals associated with the *o*-tolyl ligand were relatively independent of temperature and did not reveal any significant influence of the M≡M bond. This implied either 50:50 proximal to distal site preference for the methyl group and facile rotation about the Mo–C bond or that the *o*-tolyl ligands were aligned with their planes perpendicular to the Mo–Mo–C plane. The latter is found in the solid state and seems most likely to account for the observed ^{1}H NMR spectra.

Although we have not been able to isolate a mesityl compound 1,2-M_2($C_6H_2Me_3$)$_2$(NMe_2)$_4$ as a crystalline compound, ^{1}H NMR spectra recorded on the hexane-soluble extractions of reaction 1 employing $LiC_6H_2Me_3$ suggest that these compounds (M = Mo and W) may be formed, and if so, in solution they exist in the gauche rotamer. Moreover, only one *o*-methyl resonance signal was seen, which implies rapid (NMR time scale) rotation about the M–C (aryl) bonds.

Concluding Remarks

(1) The metal atoms in 1,2-M_2R_2(NMe_2)$_4$ compounds (M = Mo, W) have 16 valence electrons as a result of forming a M≡M bond (σ (d_{z^2}–d_{z^2}) and π (d_{xz}–d_{xz}, d_{yz}–d_{yz})), three M–L σ bonds (metal s, p_x, p_y), and two M–L π bonds (involving metal $d_{x^2-y^2}$, d_{xy}).[15] Only the metal p_z atomic orbital is not used in bonding. The characterization of the σ-benzyl complexes reported herein supports the previous conclusions concerning the stability of β-hydrogen-containing alkyl compounds M_2R_2(NMe_2)$_4$: C–H activation does not occur readily because the metal atomic orbitals are either tied up in bonding (M≡M, M—C, M=N ($\sigma + \pi$)) or apparently not suited for receiving an electron pair, as is the case for the p_z atomic orbital which lies along the M—M axis.

(2) 1,2-M_2R_2(NMe_2)$_4$ compounds exist in the ground state in conformers which have the NC_2 blades aligned along the M–M axis. In such conformers, the M–M π bonds and M–N π bonds are not in competition for use of the same metal atomic orbitals. The relatively high M–N rotational barriers[16] result from electronic factors and the marked preference for a M≡M bond in which the π bonds use d_{xz} and d_{yz} metal atomic orbitals. Computational studies, using full relaxation empirical force field (EFF) calculations, on hexaaryl ethanes reveal two potential energy minima, one corresponding to a D_3 structure composed of two essentially eclipsed homochiral triaryl propellers and the other to an S_6 structure composed of two staggered heterochiral propellers.[17] In both conformers, the dihedral angle between the C_{sp^3}–C_{sp^3}–C_{aryl} plane and the respective plane of the aryl group was ca. 50°. On purely steric grounds, similar conformational preferences would be expected for M_2(aryl)$_2$(NMe_2)$_4$ compounds.

We conclude that Me_2N-to-M π bonding produces pronounced effects in ground-state conformations, dynamic solution behavior, and reactivity patterns for the 16 valence shell electron molybdenum and tungsten compounds M_2R_2(NMe_2)$_4$. The stabilization of the 16-electron complexes relative to 18-electron complexes is presumably due to M–M σ vs. M–L bond formation (competition) in use of the d_{z^2}–p_z atomic orbitals. This preference is well illustrated by the W_2(O_2CNMe_2)$_6$ structure in which five in-plane pentagonal hybrid tungsten orbitals (s, p_x, p_y, $d_{x^2-y^2}$, d_{xy}) are used to form five strong W–O bonds (W–O = 2.1 Å (averaged)) while the sixth W–O bond, which is aligned along the W–W axis, is weak (W···O = 2.67 Å).[18]

As with other M_2X_2(NMe_2)$_4$ compounds, the physicochemical properties of the molybdenum and tungsten analogues reported here are virtually identical. The only expected structural difference of any significance is that the W≡W bond distance would be ca. 0.08 Å longer than the Mo≡Mo distance in a given aryl compound of formula 1,2-M_2(Ar)$_2$(NMe_2)$_4$.

Experimental Section

All reactions were carried out under anaerobic conditions with prepurified nitrogen and standard Schlenk and glovebox techniques. Hexane and toluene were distilled under N_2 over Na/K alloy. Glassware was flame-dried in vacuo before use. ^{1}H NMR spectra were recorded on a Varian HR 220-MHz, a Nicolet 360-MHz, or a Bruker 500-MHz NMR spectrometer, all equipped with variable-temperature probes. All spectra were run with toluene-d_8 as the solvent, with the CHD_2 protio impurity set as the reference peak at 2.09 ppm. ^{1}H NMR data are quoted in δ relative to Me_4Si and *J* in Hz. Infrared spectra were obtained from Nujol mulls between KBr plates (unless otherwise stated), using a Perkin-Elmer 283 spectrophotometer. IR data are quoted in $\bar{\nu}$ cm^{-1}. Elemental analyses were performed by Alfred Bernhardt Mikroanalytisches Laboratorium, Elbach, West Germany. Mass spectra were obtained on a Varian MS-902 by the method of direct insertion, courtesy of Peter Cook, Queen Mary College, London.

PhLi (1.9 M in 70/30 benzene/diethyl ether), BuLi (2.4 M in hexane), MeLi (1.6 M in diethylether), and all aryl bromides and iodides were purchased from Aldrich Chemical Co. Benzyllithium was synthesized by reacting ($PhCH_2$)$_3$SnCl with MeLi, as described in the literature.[19] Benzylmagnesium chloride was prepared as reported,[20] the solvent removed, and the solid residue extracted with toluene, concentrated, and crystallized.

Synthesis of Aryllithium Reagents. Lithium aryls were synthesized by reacting the appropriate aryl bromide or iodide with butyllithium in hexane. The often vigorous reaction was moderated by cooling in an ice

(14) McGlinchey, M. J. *Inorg. Chem.* **1980**, *19*, 1392.

(15) For a detailed discussion of the bonding in these types of molecules, see: Bursten, B. E.; Cotton, F. A.; Green, J. C.; Seddon, E. A.; Stanley, G. G. *J. Am. Chem. Soc.* **1980**, *102*, 4579.

(16) For a further discussion of electronic factors and Mo–N rotational barriers, see: Chisholm, M. H.; Huffman, J. C.; Rothwell, I. P. *Organometallics* **1982**, *1*, 251.

(17) Osawa, E.; Onuki, Y.; Mislow, K. *J. Am. Chem. Soc.* **1982**, *103*, 7475 and references therein.

(18) Chisholm, M. H.; Cotton, F. A.; Extine, M. W.; Stults, B. R. *Inorg. Chem.* **1977**, *16*, 603.

(19) Seyferth, D.; Suzuki, R.; Murphy, C. J.; Sabet, C. R. *J. Organomet. Chem.* **1964**, *2*, 43.

(20) Gilman, H.; Meyers, C. H. *Org. Synth.* **1925**, *4*, 59.

bath and adding the organolithium reagent over a 15-min period. A typical synthesis is described below.

Synthesis of *p*-Tolyllithium. *p*-Tolyl bromide (17.104 g, 100 mmol) was placed in a 250-mL two-necked round-bottomed flask under nitrogen and freeze–thaw degassed (3 cycles). BuLi (100 mmol, 42 mL of a 2.4 M solution in hexane) was added over 15 min while cooling the bromide in an ice bath. A yellowish solution formed, which deposited a creamy white precipitate over a 6-h period. The precipitate was collected by filtration, washed with 2 × 10 mL hexane and dried under vacuum, yield 7.36 g (75%).

Synthesis of 1,2-$Mo_2(CH_2Ph)_2(NMe_2)_4$. $Mo_2Cl_2(NMe_2)_4$[21] (500 mg, 1.14 mmol) was placed in a 100-mL round-bottomed flask with a Teflon-coated magnetic stirring bar. Toluene (50 mL) was added, and the solution cooled to −78 °C. Solid benzyl–Grignard (400 mg, excess) was added over 30 min through a solid addition tube. The reaction mixture was then warmed to room temperature and stirred for 8 h. The toluene was then stripped, hexane (50 mL) added, and the hexane solution filtered through a fine frit, yielding a dark yellow solution. Cooling at 0 °C for 3 days afforded dark yellow crystals in 60% yield (330 mg).

IR data (CsI plates): 1584 s, 1480 s, 1416 s, 1375 s, 1158 s, 1140 s, 1137 s, 1120 w, 1100 w, 1087 s, 1048 s, 1023 s, 967 w, 937 vs, 887 w, 792 s, 747 s, 690 s, 598 w, 535 w, 442 m, 395 w, 342 w, 316 w.

Mass spectrum, *m/e* 550.9 (M^+).

^1H NMR data (−75 °C, 360 MHz): 7.19 (m, Ph), 6.85 (m, Ph), 4.18, 3.53 ($[AB]_2$ spin system, CH_2 gauche rotamer, *J*(AB) = 12 Hz), 3.73 ((CH_2) antirotamer), 4.10, 3.90 (NMe, proximal, gauche rotamer), 4.07 (NMe, proximal, anti), 2.25, 2.00 (NMe, distal, gauche), 2.19 (NMe, distal, anti).

The compound 1,2-$Mo_2(CH_2C_6H_4Me\text{-}4)_2(NMe_2)_4$ was prepared in a similar fashion. Spectroscopic data are listed below.

IR data (CsI plates) 1600 m, 1503 m, 1413 m, 1372 s, 1255 m, 1235 m, 1206 w, 1186 m, 1171 w, 1142 m, 1108 m, 1073 m, 1012 m, 983 m, 938 vs, 833 w, 803 s, 727 m, 713 m, 596 w, 555 m, 530 m, 483 m, 447 m, 412 w, 331 m.

^1H NMR data (−50 °C, 220 MHz): 6.90 (m, Ph), 4.11, 3.56 ($[AB]_2$ spin system, CH_2 gauche, *J*(AB) = 12 Hz), 4.09, 3.89 (NMe, proximal, gauche), 4.05 (NMe, proximal, anti), 3.69 (CH_2, anti), 2.26, 2.19 (NMe, distal, gauche), 2.15 (NMe, distal, anti), 2.10 (C_6H_4*Me*-4, anti and gauche resonances fortuitously coincident).

Synthesis of 1,2-$W_2(CH_2Ph)_2(NMe_2)_4$. $W_2Cl_2(NMe_2)_4$[21] (1.23 g, 2 mmol) was placed in a Schlenk tube. Benzyllithium (60 mL of a 0.074 M solution in toluene/hexane, 4.44 mmol) was added. The orange solution darkened to brown within minutes as the $W_2Cl_2(NMe_2)_4$ reacted, and the solution was stirred for 2 h. The solvent was removed in vacuo and the solid residue extracted with hexane and filtered through a Celite pad and a medium porosity frit. The orange-brown solution deposited crystals when concentrated and cooled at −20 °C. Yield 81% (1.18 g).

IR data: 3065 w, 3050 w, 3010, m, 2816 m, 2770 s, 1593 m, 1570 w, 1483 m, 1448 m, 1417 m, 1390 vw, 1243 s, 1196 m, 1170 w, 1141 m, 1121 w, 1086 w, 1038 m, 1028 m, 1012 m, 989 w, 952 vs, 944 vs, 944 vs, 789 m, 750 s, 682 s.

NMR data (−45 °C, 220 MHz): 7.20–6.89 (m, Ph), 4.19, 4.02 (NMe, proximal, gauche), 4.14 (NMe, proximal, anti), 4.08, 3.31 ($[AB]_2$ spin system, CH_2 gauche, *J*(AB) = 14 Hz), 3.62 (CH_2, anti), 2.19, 1.99 (NMe, distal, gauche), 2.11 (NMe, distal, anti).

Synthesis of 1,2-$Mo_2Ph_2(NMe_2)_4$. 1,2-$Mo_2Cl_2(NMe_2)_4$ (878 mg, 2 mmol) was added to solid PhLi (4.5 mmol, 378 mg) in a Schlenk tube. Hexane (50 mL) was added and the mixture stirred magnetically for 3 h, yielding a cloudy brownish solution. Filtration through a Celite pad afforded a yellowish brown solution, which deposited dark yellow crystals when concentrated and cooled overnight at −20 °C. Yield 77% (800 mg).

IR data: 3043 m, 2814 s, 2770 s, 1420 m, 1416 m, 1393 vw, 1375 w, 1260 m, 1240 s, 1183 w, 1143 s, 1114 w, 1090 w br, 1057 w, 1046 w, 1037 m, 1016 vw, 990 w, 940 vs br, 795 m br, 730 vw, 720 s, 691 s, 659 w, 644 w, 555 w.

NMR data: (−45 °C, 220 MHz): 8.05–7.99, 7.52–7.29 (m, anti, gauche Ph), 4.10, 4.03 (NMe, proximal, gauche), 4.03 (NMe, proximal, anti), 2.57, 2.47 (NMe, distal, gauche), 2.49 (NMe, distal, anti).

1,2-$W_2Ph_2(NMe_2)_4$. Synthesized as described above for the Mo compound but with $W_2Cl_2(NMe_2)_4$.

IR data: 3045 m, 2822 m, 2780 ms, 1522 w, 1469 w, 1448 m, 1421 m, 1405 m, 1392 w, 1385 m, 1258 w, 1244 s, 1187 w, 1144 w, 1123 w, 1063 m, 1051 m, 1037 m, 1018 vw, 989 w, 955 vs, 940 vs, 800 m br, 694 s, 660 w, 650 w.

^1H NMR data (−45 °C, 220 MHz): 8.15–7.92, 7.54–7.18 (m, Ph, anti, gauche), 4.19, 4.12 (NMe, proximal, gauche), 4.10 (NMe, proximal, anti), 2.48, 2.43 (NMe, distal, gauche), 2.30 (NMe, distal, anti).

Synthesis of 1,2-$Mo_2(C_6H_4Me\text{-}2)_2(NMe_2)_4$. *o*-Tolyllithium (4 mmol, 392 mg) was placed in a Schlenk tube, followed by $Mo_2Cl_2(NMe_2)_4$ (2 mmol, 878 mg). Hexane (100 mL) was added and the suspension stirred overnight. Filtration through a medium porosity frit yielded an orange solution which precipitated large golden crystals when concentrated and cooled overnight at −5 °C. Yield 85% (620 mg).

IR data: 3043 m, 3036 m, 3029 m, 2988 w, 2823 s, 2770 s, 1566 w, 1450 m, 1434 m, 1409 m, 1390 m, 1268 w, 1257 m, 1238 s, 1190 vw, 1146 vs, 1118 vw, 1104 w, 1037 m, 1033 m, 1018 vw, 962 vw, 951 vs, 947 vs, 936 vs, 852 vw, 795 m br, 784 m, 733 s sh, 730 vs, 701 w, 658 vw, 574 w.

NMR data (−45 °C, 220 MHz): 7.91–7.86, 7.36–7.18 (m, aromatic H), 4.18, 4.10 (NMe, proximal), 2.47, 2.26 (NMe, distal), 2.14 (C_6H_4*Me*-2).

1,2-$W_2(C_6H_4Me\text{-}2)_2(NMe_2)_4$ was prepared in an analogous manner with $W_2Cl_2(NMe_2)_4$.

IR data: 3041 w, 3022 w, 2805 m, 2762 m, 1571 w, 1413 m, 1390 w, 1258 m, 1244 s, 1144 m, 1123 w, 1106 w, 1036 m, 1027 w, 949 vs, 935 vs, 797 m br, 735 vs, 707 m.

^1H NMR data (−45 °C, 220 MHz): 7.64–7.62, 7.34–7.24, 7.11–7.04 (m, aromatic CH), 4.21 (NMe, proximal), 2.27, 2.14 (NMe, distal), 1.98 (C_6H_4*Me*-2).

Synthesis of 1,2-$W_2(C_6H_4Me\text{-}4)_2(NMe_2)_4$. $W_2Cl_2(NMe_2)_4$[21] (615 mg, 1 mmol) was suspended in 40 mL of hexane. Solid LiC_6H_4Me-4 (205 mg, 2.1 mmol) was added and the solution stirred overnight, yielding a dirty brown solution. Filtration through a Celite pad removed the insoluble LiCl and any excess tolyllithium. The residue was washed with hexane (20 mL), and the washings were combined with the filtrate, yielding a reddish brown solution. Concentration in vacuo and overnight crystallization afforded a crop of reddish brown microcrystals. Yield ca. 84% (615 mg).

IR data: 3034 w, 2809 m, 2763 m, 1581 w, 1477 w, 1444 w, 1422 vw, 1392 vw, 1375 m, 1300 w, 1260 m, 1241 m, 1180 m, 1140 m, 1050 m, 1036 m, 1012 w, 951 vs, 938 vs, 795 m br, 781 s, 660 w.

^1H NMR data (−60 °C, 360 MHz): 8.02, 7.38 ($[AB]_2$ spin system, aromatic *o*- and *m*-H, anti, *J*(AB) = 9 Hz), 7.98, 7.27 ($[AB]_2$ spin system, aromatic *o*- and *m*-H, gauche, *J*(AB) = 8 Hz), 4.25, 4.16 (NMe, proximal, gauche), 4.18 (NMe, proximal, anti), 2.54, 2.43 (NMe, distal, gauche), 2.50 (NMe, distal, anti), 2.32 (C_6H_4*Me*-4, anti), 2.26 (C_6H_4*Me*-4, gauche).

1,2-$Mo_2(C_6H_4Me\text{-}4)_2(NMe_2)_4$ was made in similar fashion to the tungsten analogue, employing $Mo_2Cl_2(NMe_2)_4$.[21]

IR data: 3027 w, 3014 w, 2809 m, 2764 m, 1580 w, 1479 w, 1445 m, 1414 m, 1393 vw, 1300 vw, 1258 m, 1236 m, 1180 m, 1140 m, 1088 w br, 1045 m, 1038 m, 1015 vw, 949 s, 938 vs, 796 m, 783 s, 658 w.

^1H NMR data (−80 °C, 500 MHz): 8.01, 7.19 ($[AB]_2$ spin system, aromatic *o*-, *m*-H, gauche, *J*(AB) = 8 Hz), 7.99, 7.32 ($[AB]_2$ spin system, aromatic *o*-, *m*-H, anti, *J*(AB) = 8 Hz), 4.16, 4.08 (NMe, proximal, gauche), 4.07 (NMe, proximal, anti), 2.62, 2.53 (NMe, distal, gauche), 2.55 (NMe, distal, anti), 2.33 (C_6H_4*Me*-4 , anti), 2.26 (C_6H_4*Me*-4, gauche).

Reaction of Mesityllithium with 1,2-$W_2Cl_2(NMe_2)_4$. 1,2-$W_2Cl_2(NMe_2)_4$[21] (615 mg, 1 mmol) was suspended in hexane (30 mL). Mesityllithium ($LiC_6H_2Me_3$-2,4,6, 252 mg, 2 mmol) was added and the solution stirred for 3 days. The brownish solution was then filtered; the residue appeared to contain unreacted 1,2-$W_2Cl_2(NMe_2)_4$ in addition to LiCl. The red filtrate was concentrated and a few crystals of 1,2-$W_2Cl_2(NMe_2)_4$ formed. No further products could be crystallized, oils being formed on further concentration. The oily red product was pumped for 2 days under high vacuum, yielding a reddish brown solid. ^1H NMR spectroscopy suggested the presence of 1,2-$W_2(C_6H_2Me_3\text{-}2,4,6)_2(NMe_2)_4$, together with other uncharacterized compounds. Repeated attempts to purify and isolate this compound, for both molybdenum and tungsten, were unsuccessful.

X-ray Structural Determinations. General procedures have been described previously.[22]

1,2-$Mo_2(CH_2C_6H_5)_2(NMe_2)_4$. A yellow crystal of dimensions 0.18 × 0.18 × 0.24 mm was cleaved from a larger crystal, mounted in a nitrogen-filled glovebag, and transferred to the liquid nitrogen boiloff system of the diffractometer, where cell dimensions were obtained at −165 °C. The space group was found to be $P2_1/a$ with a = 17.595 (7) Å, b = 16.038 (6) Å, c = 10.542 (4) Å, β = 122.11 (2)°, V = 2519.81 Å^3, Z = 4, d_{calcd} = 1.451 g cm^{-3}, using Mo Kα (λ = 0.71069 Å), μ = 9.854.

Data were collected at −165 °C. Of a total of 5121 reflections, 4431 unique reflections were measured, using moving-crystal, moving-counter techniques. The scan speed = 4.0 deg min^{-1}; scan width = 1.8 + dispersion; single background time at extremes of scan = 5 s; aperture size

(21) Akiyama, M.; Chisholm, M. H.; Cotton, F. A.; Extine, M. W.; Murillo, C. A. *Inorg. Chem.* **1977**, *16*, 2407.

(22) Huffman, J. C.; Lewis, L. N.; Caulton, K. G. *Inorg. Chem.* **1980**, *19*, 2755.

= 3.0 × 4.0 mm. A total of 3666 reflections had $F > 2.33\sigma(F)$; these were used in the refinement. The limits of data collection were $5° < 2\theta < 50°$.

The structure was solved using conventional Patterson and Fourier techniques. Refinement, using standard full-matrix least-squares cycles, located all atoms including hydrogens. These were refined isotropically while all other atoms were refined anisotropically. Refinement converged at $R(F) = 0.036$, $R_w(F) = 0.038$. The goodness of fit for the last cycle was 1.012, while the maximum $\Delta/\sigma = 0.10$.

1,2-$Mo_2(C_6H_4Me\text{-}4)_2(NMe_2)_4$. The sample used in the study was cleaved from a larger needle and transferred to the goniostat, using standard inert atmosphere handling techniques. Data were collected at −162 °C and yielded the following cell dimensions from a reciprocal-space search: space group = *Pcan*, a = 8.046 (2) Å, b = 17.319 (7) Å, c = 18.179 (8) Å, V = 2533.2 Å^3, Z = 4, d_{calcd} = 1.443 g cm^{-3}, using Mo Kα (λ = 0.71069 Å), μ = 9.802, scan speed = 4.0 deg min^{-1}, scan width = 2.0 + dispersion, single background at extremes of scan = 5 s, aperture size = 3.0 × 4.0 mm, $5° < 2\theta < 50°$.

Of a total of 3688 reflections, 2250 were unique, and 1864 had $F > 2.33\sigma(F)$; the latter were used in refinement. The structure was solved by direct methods and refined by full-matrix least squares, using isotropic thermal parameters for hydrogens. The structure converged at $R(F)$ = 0.038, $R_w(F)$ = 0.026, there being no peak greater than 0.42 electron Å^{-3} in the final difference Fourier map. The goodness of fit for the last cycle was 3.397, while the maximum $\Delta/\sigma = 0.05$.

1,2-$Mo_2(C_6H_4Me\text{-}2)_2(NMe_2)_4$. Golden crystals of the titled compound were grown from hexane. A crystal was mounted on the diffractometer as described for the previous structures. Cell dimensions and data were collected at −161 °C and are as follows: space group $A2/a$, a = 16.845 (4) Å, b = 17.651 (5) Å, c = 8.451 (2) Å, β = 102.74 (1)°, V = 2451.0 Å^3, Z = 4, d_{calcd} = 1.492 g cm^{-3}, using Mo Kα radiation (λ = 0.71069 Å), μ = 10.130, scan speed = 3.0 deg min^{-1}, scan width = 2.0 + dispersion, single background time at extremes of scan = 5 s, aperture size = 3.0 × 6.0 mm.

The total number of reflections collected was 2568 with $5° < 2\theta < 50°$. Out of 2171 unique intensities, 1892 had $F > 2.33\sigma(F)$; these were used in solving the structure. The position of all atoms was determined by using direct methods and full-matrix least squares. Hydrogen atoms were refined isotropically, while for all other atoms anisotropic thermal parameters were used. Refinement converged at $R(F)$ = 0.033, $R_w(F)$ = 0.023, with the goodness of fit for the last cycle being 2.981 and the maximum $\Delta/\sigma = 0.05$. A final difference Fourier synthesis was featureless, the largest peak being 0.45 electron Å^{-3}.

Acknowledgment. We thank the Office of Naval Research and the Wrubel Computing Center for support of this work.

Registry No. 1,2-$Mo_2(CH_2Ph)_2(NMe_2)_4$, 82555-51-9; 1,2-$W_2(CH_2Ph)_2(NMe_2)_4$, 82555-52-0; 1,2-$Mo_2(CH_2C_6H_4Me\text{-}4)_2(NMe_2)_4$, 84417-29-8; 1,2-$Mo_2Ph_2(NMe_2)_4$, 84417-24-3; 1,2-$W_2Ph_2(NMe_2)_4$, 84417-25-4; 1,2-$Mo_2(C_6H_4Me\text{-}2)_2(NMe_2)_4$, 84417-23-2; 1,2-$W_2(C_6H_4Me\text{-}2)_2(NMe_2)_4$, 84417-27-6; 1,2-$Mo_2(C_6H_4Me\text{-}4)_2(NMe_2)_4$, 84417-22-1; 1,2-$W_2(C_6H_4Me\text{-}4)_2(NMe_2)_4$, 84417-28-7; 1,2-$W_2(C_6H_2Me_3\text{-}2,4,6)_2(NMe_2)_4$, 84417-26-5; $Mo_2Cl_2(NMe_2)_4$, 63301-82-6; $W_2Cl_2(MMe_2)_4$, 63301-81-5; $C_6H_5CH_2Cl$, 100-44-7; *p*-tolylCH_2Cl, 106-43-4; BuLi, 109-72-8; PhLi, 591-51-5; *p*-tolyllithium, 2417-95-0; *p*-tolyl bromide, 106-38-7; benzyllithium, 766-04-1; *o*-tolyllithium, 6699-93-0; mesityllithium, 5806-59-7.

Supplementary Material Available: Tables of observed and calculated structure factor amplitudes and anisotropic thermal parameters for the 1,2-$M_2R_2(NMe_2)_4$ compounds where R = $CH_2C_6H_5$, C_6H_5Me-2, and C_6H_5Me-4 (62 pages). Ordering information is given on any current masthead page.

Protonation Equilibria in Excited-State Tris(bipyrazine)ruthenium(II)

R. J. Crutchley,* N. Kress, and A. B. P. Lever*

Contribution from the Department of Chemistry, York University, Downsview, Ontario, Canada M3J 1P3. *Received June 17, 1982*

Abstract: The tris(bipyrazine)ruthenium(II) cation has six peripheral uncoordinated nitrogen atoms potentially available for protonation in acidic media. Studies of the absorption and emission spectroscopy of the ruthenium cation in media ranging from neutral water to concentrated sulfuric acid show that it is, indeed, possible to sequentially protonate these six nitrogen atoms. As the acidity is increased, a series of isosbestic points are seen in the absorption spectra, and these shift as the equilibria change upon increasing acidity. The parallel studies of emission show six different protonated species with distinct emission maxima and lifetimes ranging from 27 to 520 ns. The first three protonation steps, to three different bipyrazine rings on the cation, have MLCT excited states that are stronger bases than the ground state, while for the second set of three protonation species, the MLCT excited states are weaker bases than the ground state. pK_a and pK_a^* values for many of the species are reported. Protonation equilibria with the free base bipyrazine are also included.

During the past 15 years there has been great activity studying the ground- and excited-state chemistry of the $Ru(bpy)_3^{2+}$ cation (I) (bpy = 2,2′-bipyridine). Of particular relevance have been studies of the excited-state photochemistry and photophysics of this species with a view to developing solar energy conversion catalysts. The area is the subject of a recent review.[1] The considerable effort expended on this species has also contributed greatly to our understanding of the chemistry of inorganic molecules in their excited states.

The analogous $Ru(bpz)_3^{2+}$ cation (II) (bpz = bipyrazine) has also been shown[2] to be an excellent photocatalyst, complementary in many ways to species I. In a detailed study of bipyrazine metal complexes,[2] the redox couples were shown, generally, to be shifted ca. 0.5 V positive relative to corresponding couples in corresponding bipyridine complexes. This positive shift was seen to be due to much reduced σ bonding strength in the bipyrazine, relative to the bipyridine derivatives.

Thus the bipyrazine complexes have the potential to be better oxidizing photocatalysts than their bipyridine analogues. There is considerable interest in generating photocatalysts capable of photooxidizing water or halogen ions, hence our continuing interest in these bipyrazine species. The existence of uncoordinated nitrogen atoms on the periphery of species II not only provides a possible mechanism for coupling a substrate molecule to the excited photocatalyst but also, via protonation, can be expected to yield species with even more positive oxidizing potentials.

In this paper, we report spectrophotometric absorption and emission studies performed both on free bipyrazine and on the

(1) Kalyanasundarum, K. *Coord. Chem. Rev.* **1979**, *46*, 159–244.
(2) Crutchley, R. J.; Lever, A. B. P. *J. Am. Chem. Soc.* **1980**, *102*, 7128–7129; *Inorg. Chem.* **1982**, *21*, 2276–2282.

0002-7863/83/1505-1170$01.50/0 © 1983 American Chemical Society